Available online at www.sciencedirect.com
SCIENCE DIRECT®
Surface Science 575 (2005) 171–180
SURFACE SCIENCE
www.elsevier.com/locate/susc

Hydrogen adsorption on β-Ga_2O_3(100) surface containing oxygen vacancies

Estela A. Gonzalez [a], Paula V. Jasen [a], Alfredo Juan [a,*], Sebastián E. Collins [b], Miguel A. Baltanás [b], Adrian L. Bonivardi [b]

[a] *Departamento de Física, Universidad Nacional del Sur, Av. Alem 1253, Bahía Blanca 8000, Argentina*
[b] *Instituto de Desarrollo Tecnológico para la Industria Química, Güemes 3450, Santa Fe 3000, Argentina*

Received 6 August 2004; accepted for publication 10 November 2004
Available online 28 November 2004

Abstract

The understanding of hydrogen (H) adsorption on gallia is an important step in the design of molecular sensors and alkane dehydrogenation–aromatization catalysts. We have simulated the (100) surface of β-Ga_2O_3, which is the more frequent cleavage plane. Our study has considered oxygen vacancies in that plane. We have used the atom superposition and electron delocalization molecular orbital (ASED-MO), a semiempirical theoretical method, to understand both the electronic and bonding characteristic of H on β-Ga_2O_3 surface. As a surface model, we have considered both a cluster and a five-layer slab. We have found that H adsorption occurs on Ga sites close to oxygen vacancies.

Two types of Ga have also been considered; namely, Ga(I) and Ga(II), with different coordination: Ga(I) is four-coordinated and Ga(II) six-coordinated. The Ga(I)–H bond is ∼24% stronger than Ga(II)–H while Ga(I)–O(I) bond is ∼44% stronger than Ga(II)–O(I). Also, Ga(I)–O(III) is ∼56% stronger that Ga(II)–O(III). The Ga–H and Ga–O interactions are always bonding. The Ga–Ga overlap population is null.

We have assigned the 2003 and 1980 cm^{-1} infrared bands to the stretching frequencies of Ga(I)–H and Ga(II)–H bonds, respectively.

Keywords: Gallium oxide; Hydrogen adsorption; Theoretical calculation

1. Introduction

The stable form of gallia from room temperature to its melting point is β-Ga_2O_3 [1]. This material belongs to the group of transparent conductive oxides (TCO) with a large band gap (4.8 eV) and

* Corresponding author. Tel./fax: +54 291 4595142.
E-mail address: cajuan@criba.edu.ar (A. Juan).

0039-6028/$ - see front matter © 2004 Elsevier B.V. All rights reserved.
doi:10.1016/j.susc.2004.11.018

electrical conductivity (σ)—that at high temperature is proportional to the—1/4-th power of the oxygen partial pressure in the surrounding gas [2,3]. The electrical conductivity of the TCO's is attributed to the existence of oxygen vacancies, which is caused by the tendency of all these oxides to deviate from the stoichiometric composition.

The amount of oxygen vacancies can induce a change in the electrical character of the specimens. The β-Ga_2O_3 can vary from insulating to conductive [4–6]. However, it is generally an n-type semiconductor due to oxygen vacancies individually compensated by two electrons, forming shallow donors with ionization energy $E_d \approx 0.03$–0.04 eV [4]. The electrical conductivity of the β-Ga_2O_3 crystals exhibits a semiconductor behavior even at very low temperature.

Polycrystalline semiconducting Ga_2O_3 thin films represent a promising material for sensors devices to detect molecular hydrogen [7–9], and catalysts containing supported gallium are known to be active in light alkane dehydrogenation and/or aromatization (Cyclar process) [10–12]. Recently, Collins et al. have highlighted that β-Ga_2O_3 alone is able to dissociate hydrogen molecules at temperatures higher than 500 K and then hydrogenate adsorbed CO_2 stepwise from formate to methoxy groups [13]. Even though the oxidation state of gallium ions has been of a matter of debate in catalytic reactions [11,14,15], the role of the geometric environment or coordination of surface gallium–hydrogen sites has not been emphasized.

Experimental results by Cooper et al. [16] have shown that doping β-Ga_2O_3 with low levels of zinc promotes the activity for methane oxidation and it has been proposed that this is due to an increase of the defect concentration in the catalyst. Conversely, the addition of magnesium suppressed the activity. Those studies, which have combined experimental and theoretical approaches, probed the relationship between the Ga_2O_3 structure, its chemistry and the ability to activate methane [16]. It seems that oxygen vacancies should be considered as a part of a model of an active gallia surface.

At a given temperature, ranging from 873 to 1173 K the desorption of CO results in the formation of oxygen vacancies at the (1 0 0) surface. Thus, the interaction with methane is possible being Ga_2O_3 a suitable material for detection of oxidizable gases [17,18].

In addition, and on powder catalysts, several workers have highlighted the need of coordinative unsaturated (cus) Ga^{3+} ions (oxygen vacancies) over the surface of different unsupported and supported gallium oxides to allow the adsorption of CO to take place. For instance, Otero Areán's group [19–21] found that CO is adsorbed on cus Ga^{3+} sites on the surface of α, β and γ-Ga_2O_3 after their thermal activation at 673 K under vacuum. More recently, Kazansky et al. [22] have concluded that their DRIFT spectra of adsorbed of CO on 5% Ga/ZSM-5, which was activated at 773 K in vacuo, gave insight into cusgallium species. Then, surface oxygen vacancies on various forms of activated gallium oxides permit the adsorption of carbon monoxide on cusGa^{3+} sites. Similarly, Collins et al. [15] put forward that the hydrogen adsorption on silica-supported gallium oxide is due to the interaction of H_2 molecules over 'bare' partially reduced gallium cations in gallium oxide patches.

The electronic structure of β-Ga_2O_3 shows that the conduction band has a strong Ga 4*s* character (≈60%) with quasi-exclusive contribution of the octahedral Ga ions to the band edge [23]. Conductions electrons are essentially delocalized along the octahedral chains of the structure whereas the surrounding tetrahedral chains are not occupied.

The aim of this paper is to study the electronic structure and bonding of β-Ga_2O_3(1 0 0) and the H-surface bonds which could be established after adsorption and relate the theoretical results to ours experimental data of H_2 chemisorption on Ga_2O_3.

2. Experimental data

β-Ga_2O_3 phase was synthesized following a procedure similar to that reported by Otero Areán and co-worker [19]. Hydrated gallium hydroxide gel was obtained from the addition of an ammonia ethanolic solution (50% v/v) to 7 wt.% $Ga(NO_3)_3 \cdot xH_2O$ (Strem Chemicals, 99.99% Ga) in ethanol. This gel was filtered under vacuum and washed with ethanol at room temperature until no NO_3^- anions were detected in the washing solution by

UV spectroscopy. The washed gel was then dried at 343 K (1 h) and next calcined in air at 923 K (6 h). The crystallographic phase of the resulting β-Ga_2O_3 oxide was verified by X-ray diffraction spectrometry (XRD) using a Shimadzu XD-D1 apparatus (Cu Kα radiation) and the measured Brunauer–Emmett–Teller surface area (S_{BET}, N_2 adsorption at 77 K) was equal to 64 m^2/g.

A self-supported wafer of the gallia sample of 13 mm of diameter was made by pressing 30 mg of powder at 5 ton cm^{-2}. This wafer was placed into an infrared Pyrex® cell with water-cooled NaCl windows, which was attached to a conventional manifold system as previously described [24]. To eliminate the artificial bands in the 3000–2800 cm^{-1} region that arise from oil contamination during wafer preparation, which are attributed to the C–H stretching modes [15], an in situ cleaning pretreatment of the wafer had to be performed before the hydrogen adsorption–desorption experiments took place, by: (a) heating under O_2 (100 $cm^3 min^{-1}$, 5 K min^{-1}) from 298 to 723 K; and then (b) cooling down to 298 K under vacuum (base pressure = 1.33×10^{-4} Pa). After the cleaning procedure, the sample was heated from 298 K to 723 K (5 K min^{-1}) flowing H_2 (100 $cm^3 min^{-1}$) through the cell at atmospheric pressure (101.3 kPa). Next, a mixture of H_2/D_2 = 1/1 v/v (100 $cm^3 min^{-1}$) was admitted into the IR cell for 15 min and, finally the gas flow was switched to pure D_2 for another 15 min (100 $cm^3 min^{-1}$) at 723 K.

In situ infrared spectra were recorded by a Shimadzu 8210 FT-IR spectrometer using a DLATGS detector (4 cm^{-1} resolution, 100 scans). The spectra were further processed by employing the Microcal Origin® 4.1 software (with Peak fitting module): background correction of the spectra was achieved by subtracting the spectra of the 'clean wafers' at each temperature; and a Lorentzian sum function was used for fitting the overlapped bands and measuring peak areas [25].

3. Surface model

From the structural standpoint, β-Ga_2O_3 is monoclinic with space group C2/m and with lattice parameters a = 12.23 Å, b = 3.040 Å, c = 5.807 Å, and β = 103.7° [26]. There are four Ga_2O_3 in the unit cell. The lattice is composed of two types of coordination for Ga^{3+} ions in this structure, namely tetrahedral and octahedral—hereafter referred to as Ga(I) and Ga(II)—and three types of oxygen ions, referred to as O(I), O(II) and O(III). Oxygen O(I) and O(II) lie respectively in and out of the symmetry plane (see Fig. 1a). They are both in threefold coordination while O(III) is in fourfold coordination [23]. The β-Ga_2O_3 structure is made up of double chains of edge-sharing octahedra running along the b-axis (see Fig. 1b). These chains are linked to single chains of tetrahedra along b in such a way that six tetrahedral chains surround each double octahedral chain. Therefore, a given gallium is surrounded by many closely spaced neighbors either in octahedral or in tetrahedral sites. The oxygen ions are arranged in a "distorted cubic" close-packed array. Because of the short b-axis, there are two $O(I)^{2-}$ and two $O(III)^{2-}$ ions (along the b-axis) at the corners of an octahedron. The structure cannot possibly then have two $O(II)^{2-}$ ions at the remaining corners of

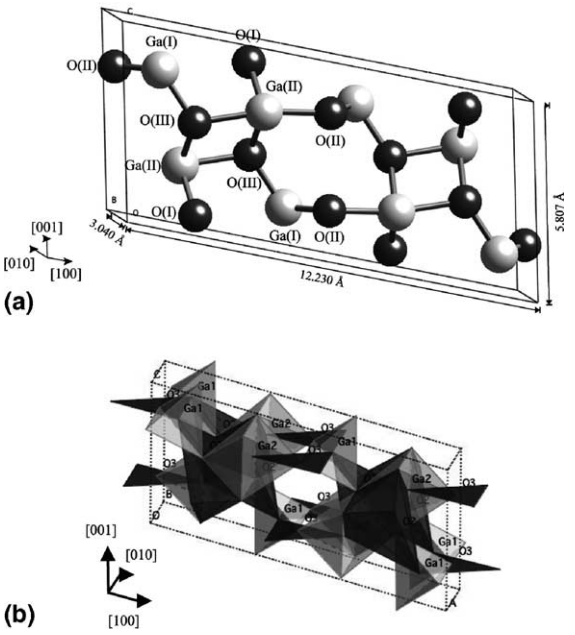

Fig. 1. (a) Crystal structure of β-Ga_2O_3 unit cell. (b) Crystal structure of β-Ga_2O_3, tetrahedral and octahedral chains views.

the octahedron, since these must lie in the mirror plane containing the $Ga(II)^{3+}$ ion within the octahedron. Thus, there is only one $O(II)^{2-}$ ion at a corner of the octahedron the remaining corner being occupied by a third $O(III)^{2-}$ ion. At the corners of the tetrahedron, there are two $O(II)^{2-}$ ions which are along the *b*-axis, the other corners are occupied by an $O(I)^{2-}$ and an $O(III)^{2-}$ in each lying in the mirror plane containing the $Ga(I)^{3+}$ ion within the tetrahedron. If the octahedra and tetrahedra were regular, it would be doubtful that such a structure could exist because the sums of the bond number of the bonds at all oxygen ions would not be two [27].

β-Ga_2O_3 presents two cleavage planes, the more frequent is the (1 0 0) plane, and the secondary the (0 0 1). The first correlates with the O(II) sites, while the second with the O(I) and O(III) sites, indicating clearly the order of bonding strength, that varies from O(III), O(I) to O(II) (also from higher to lower coordination). The lattice expansion coefficient ($4.2\times10^{-6}\,K^{-1}$) along the *b* and *c* axes is three times larger than that ($1.4\times10^{-6}\,K^{-1}$) along the *a*-axis, indicating that the lattice expansion takes place mainly in the (1 0 0) plane [6]. Moreover, the (1 0 0) plane is mainly formed by oxygen.

We simulate the (1 0 0) plane growing along the *b* and *c* axes. Our calculations were done in an extended model (see Fig. 2). The slab is composed by the half of the β-Ga_2O_3 unit cell shown in Fig. 1a. As mentioned before, this plane is not reactive unless the composite receives energy or some oxygen vacancies are generated.

For this reason, the adsorption process was conducted having O(II) vacancies in order to provide adsorption sites for the adsorbates (see Fig. 2b). The lowest formation energy belongs to the threefold coordinated vacancies in the neutral, O(II), and to the fourfold coordinated O-vacancy in its double positive state. High temperature n-type conduction in β-Ga_2O_3 is explained on the basis of thermal equilibrium of these two-vacancy sites [28].

The process itself is comprised by two separated cases. In the first case, the H was adsorbed on a Ga(I) site and in a second case to a Ga(II) site (see Fig. 3). Even in presence of oxygen vacancies, the adsorption of H on the remaining oxygen (of the second layer) is not energetically stable.

4. Results and discussion

4.1. Ga_2O_3 surface

The crystal electronic states are separated in two groups. States between −13 and −17 eV are mainly O 2p while states between −28 and −30.6 eV are originated from O 2s. The oxygen ions contribute equally to the total density of states (DOS), though these coordination's numbers are different (O(I), O(III)). The Ga (I or II) contribution to the DOS is much lower. Both regions contain Ga 4s and Ga 4p orbitals being more

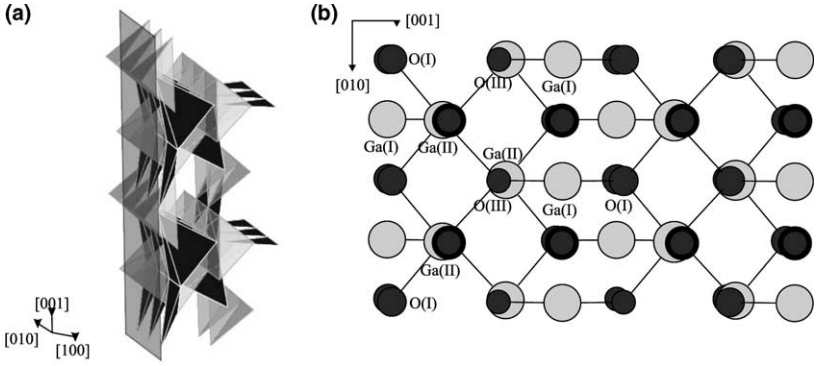

Fig. 2. Lateral, octahedral and tetrahedral coordination (a), and top (b) view of (1 0 0) plane. () Superficial oxygen O(II) to be removed before H absorption.

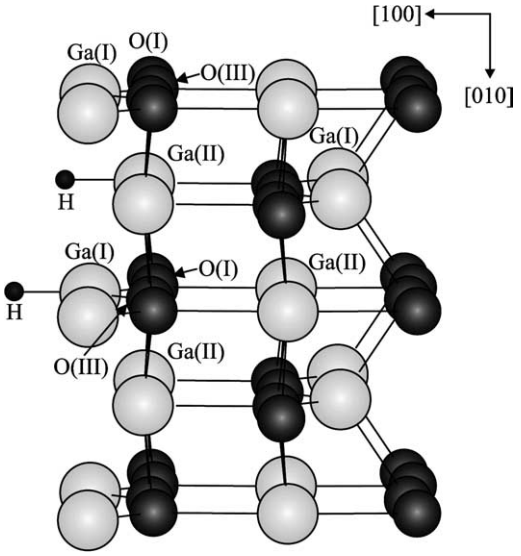

Fig. 3. Lateral view of the β-Ga_2O_3 with oxygen's vacancies after H adsorption on Ga(I) and Ga(II) sites.

p in character near to the Fermi level (E_F = −13.43 eV).

The electron density, charge, overlap population (OP) and distances for the bonds indicated in Fig. 2b are briefly reported in Table 1. The obtained Ga–O OP is similar to that reported by Binet et al. [23] and there no Ga–Ga bonds are found. The Ga–O OP values change with the coordination number of the atoms involved being the Ga(I)–O(I) OP higher than the others (see Table 1). The crystal orbital overlap population (COOP) analysis shows that all Ga–O interactions are bonding in the energy windows.

4.2. Ga_2O_3 surface with O-vacancies

The electronic structure data are presented in Table 1 for an oxygen vacancy containing β-Ga_2O_3(1 0 0) plane (see the structure in Fig. 2b for notation). The oxygens in Ga(II)–O(I) and Ga(II)–O(III) bonds gained some electronic charge while the both galliums become slightly more positive. There is also more bonding Ga(I)–O(I) (0.406 vs. 0.367) and Ga(I)–O(III) (0.329 vs. 0.368) when compared with the solid without oxygen vacancies.

The DOS plots look similar for the projections of different oxygens with some differences for the Ga(II) peak at ≈−17 eV, which is more developed. In addition, new Ga based states are present above the Fermi level (E_F = −13.42 eV).

The Ga–O COOP curves are also similar to that of the perfect solid with a peak at −10 eV, which is antibonding but not populated (see Fig. 4b). The Ga–Ga interactions are all antibonding. The bonding composition is mainly due to Ga 4p–O 2p orbitals and Ga 4s with O $2p_z$ interactions.

4.3. H adsorption on Ga_2O_3 surface

The H is adsorbed on the Ga atoms on the surface with O(II) vacancies (see Fig. 3); thus, no bonding interaction is developed with oxygen. Table 1 shows that the O–H OP is almost null. After H adsorption the E_F = −13.40 eV.

After H adsorption, the Ga(I)–O OP decreases 15% and, Ga(II)–O(I) and Ga(II)–O(III) OPs decreases 22% and ∼24% respectively while a strong Ga–H bond is formed (see Fig. 4c). The Ga–H adsorption distances are ∼1.147 Å, which is shorter than distances in Ga–H compounds. In Ga_2H_2, Himmel et al. have reported Ga–H distances of about 1.6 Å [29] and for digallane (Ga_2H_6) the terminal hydrogen is a 1.52 Å from Ga [30,31].

When H is adsorbed, the composition of Ga(II)–H bond includes Ga 4s–H 1s interactions of about 80% and Ga $4p_x$–H 1s (20%). In the case of Ga(I)–H, the composition is 73% and 27%, respectively. The OP of H on Ga(I) is 24% higher than on Ga(II) while Ga(I)–O(I) OP is 44% higher than Ga(II)–O(I). Ga(I)–O(III) OP is 56% higher that Ga(II)–O(III) (see Fig. 4a and b).

The DOS is similar to that of Ga_2O_3 surface with oxygen vacancies, except for a peak at −17.9 eV (Ga(I)) and −17.6 eV (Ga(II)) formed by H contribution. The H on Ga(I) is 0.95 eV lower in energy that is consistent with its higher OP and stability.

The Ga(II)–Ga(I) interaction is almost antibonding while Ga(I)–Ga(I) present a very slightly bonding character (see Table 1). Ga–H and Ga–O interactions are always bonding as shown in Fig. 4 and the Ga–H bond is formed at expenses of Ga–O. Ga(II)–O(I), Ga(II)–O(III) OP decreases from 0.245 and 0.178 to 0.191 and 0.136 respectively

Table 1
Electron density, overlap population, charge and distances for the β-Ga_2O_3(100) surface, pure with O(II)-type vacancies and after H adsorption

Structure		Electron density			Charge	OP[a]	Distances (Å)
		s	p	d			
β-*Ga_2O_3 (Ga(II))*[b]							
Ga(II)–O(I)	Ga(II)	0.92	0.44	0.00	1.636	0.245	1.979
	O(I)	1.95	5.66	0.00	−1.609		
Ga(II)–O(III)	O(III)	1.86	4.89	0.00	−0.753	0.178	2.024
β-*Ga_2O_3 (Ga(I))*[b]							
Ga(I)–O(I)	Ga(I)	0.97	0.30	0.00	1.749	0.406	1.805
	O(I)	1.83	4.80	0.00	−0.634		
Ga(I)–O(III)	O(III)	1.84	4.81	0.00	−0.650	0.368	1.833
β-*Ga_2O_3–H (Ga(II))*[c]							
Ga(II)–H	H	0.82	0.00	0.00	0.183	0.627	1.137
	Ga(II)	0.91	0.56	0.00	1.528		
O(I)–H	O(I)	1.95	5.40	0.00	−1.358	0.013	2.334
O(III)–H	O(III)	1.86	4.77	0.00	−0.632	0.006	2.444
Ga(II)–Ga(I)	Ga(I)	0.89	0.43	0.00	1.672	0.000	3.277
Ga(II)–Ga(II)	Ga(II)	0.92	0.44	0.00	1.636	0.000	3.040
Ga(II)–O(I)	O(I)	1.95	5.40	0.00	−1.358	0.191	1.979
Ga(II)–O(III)	O(III)	1.86	4.77	0.00	−0.632	0.136	2.024
β-*Ga_2O_3–H (Ga(I))*[c]							
Ga(I)–H	H	1.02	0.00	0.00	−0.025	0.776	1.147
	Ga(I)	0.96	0.52	0.00	1.524		
O(I)–H	O(I)	1.83	4.67	0.00	−0.506	0.000	2.582
O(III)–H	O(III)	1.84	4.59	0.00	−0.440	0.000	2.642
Ga(I)–Ga(I)	Ga(I)	0.97	0.30	0.00	1.751	0.002	3.040
Ga(I)–Ga(II)	Ga(II)	0.87	0.54	0.00	1.587	0.000	3.279
Ga(I)–O(I)	O(I)	1.83	4.67	0.00	−0.506	0.346	1.805
Ga(I)–O(III)	O(III)	1.84	4.59	0.00	−0.440	0.312	1.833

[a] The OP for the different Ga–O bonds in the bulk are Ga(II)–O(I): 0.227; Ga(II)–O(III): 0.164; Ga(I)–O(I): 0.367; Ga(I)–O(III): 0.329.
[b] As shown in Fig. 2b.
[c] As shown in Fig. 3.

while Ga(I)–O(I) and Ga(I)–O(III) change from 0.406 and 0.368 to 0.346 and 0.312 respectively.

Fig. 4 shows that Ga(I)–H interactions are more bonding in character than Ga(II)–H interactions.

4.4. H_2 adsorption on β-Ga_2O_3 by IR spectroscopy

Infrared spectra collected during the heating procedure under H_2 gas revealed the evolution of two partially convoluted IR signals at 2003 and 1980 cm^{-1} from 473 K onwards. The origin of these bands has been attributed to gallium–hydrogen bond formation and was previously assigned to the stretching mode of Ga–H, ν(Ga–H) [15]. Fig. 5 shows the thermal evolution of the total integrated absorbance of the ν(Ga–H) bands. Both bands developed gradually, together, to reach a plateau from 673 K. Additionally, a broad band around 3500 cm^{-1}, and assigned to the stretching mode of O–H bonded to Ga sites [ν(GaO–H)], decreased owing to a partial dehydroxylation (and/or reduction) of the gallium oxide surface leaving cus Ga surface sites as in the case on supported gallium oxide on silica [15].

The infrared spectra of the H–D exchange experiment at 723 K are summarized in Fig. 6.

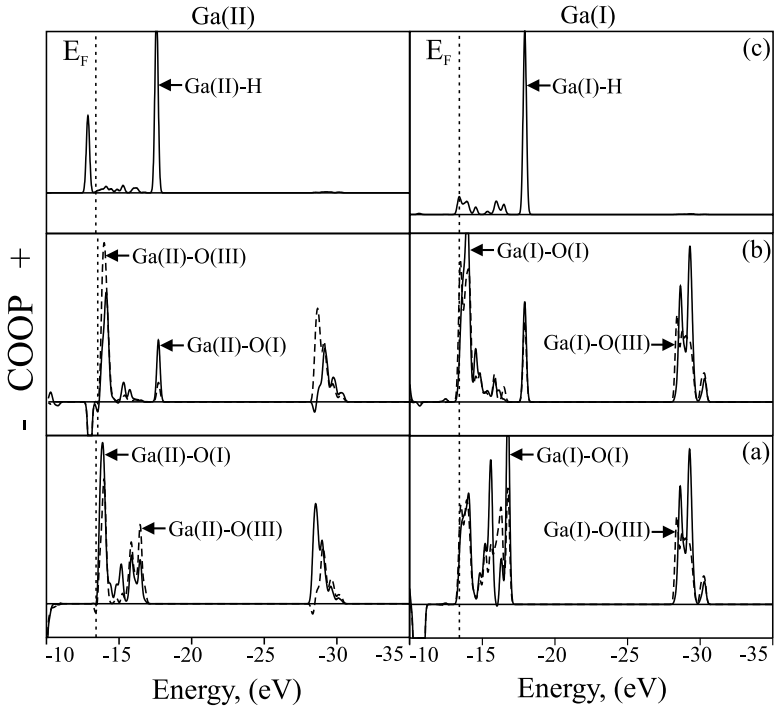

Fig. 4. COOP curves for Ga–O interaction before (a) and after H adsorption (b). The Ga–H COOP are also shown (c).

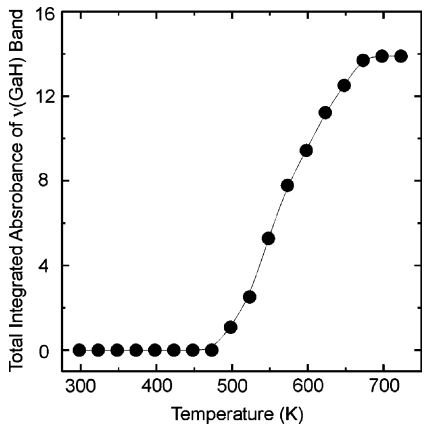

Fig. 5. Total integrated absorbance of the ν(Ga–H) bands vs. temperature.

After switching form H_2 to a H_2/D_2 equimolar mixture, a decrease in the intensity of the $\sim$2000 cm^{-1} bands is observed while new bands at 1440 and 1416 cm^{-1} show up. Under pure D_2, only the $\sim$1420 cm^{-1} peaks remain on the material. The experimental values for the ratios between these wavenumbers are 1.39 and 1.40 respectively, which are the expected ones for the ν(Ga–H) vs. the ν(Ga–D) modes, i.e. 1.40.

The formation of $Ga^{\delta+}$–H species ($\delta < 2$) was previously identified and characterized by means

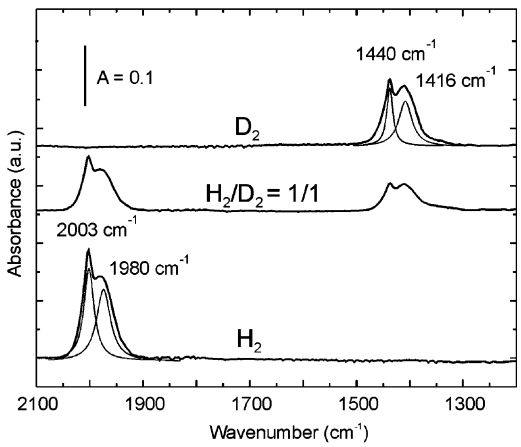

Fig. 6. Infrared spectra of the H–D exchange experiment at 723 K.

of infrared and X-ray photoelectron spectroscopies on silica-supported gallium oxide [15]. Hence, based on those findings and the present results, it is possible to postulate that H_2 molecule is dissociatively chemisorbed over the β-Ga_2O_3 surface above 500 K, producing terminal Ga–H species on the surface with stretching frequencies at 2003 and 1980 cm^{-1}. However, the assignment of both signals coming from Ga–H bonds is not obvious.

The position of these bands cannot be attributed to the naturally occurring isotopes Ga^{69} (60.1%) and Ga^{71} (39.9%) because the difference between the wavenumbers for $\nu(Ga^{69}–H)$ and $\nu(Ga^{71}–H)$ should be about 1 cm^{-1}, instead of the 23 cm^{-1} observed in our spectra.

To explain the appearance of two bands at 2000 cm^{-1}, it is also possible to invoke the formation of Ga–H–Ga, H–Ga–OH or H–Ga–H like bonds. Yet, in Ga–H–Ga bridges, the antisymmetric and symmetric stretching frequencies usually lie under ~1700 cm^{-1}, i.e. far away below 2000 cm^{-1} [29,31–34]. Therefore, more probably the Ga–H–Ga bond formation should be ruled out and a similar conclusion is applicable for the H–Ga–OH species formation, which has a stretching ν(Ga–H) band at 1670 cm^{-1} [32,34,35].

However, Pulham et al. reported two terminal hydrogen vibrational bands in digallane [H_2Ga- (μ-H_2)GaH_2]: 1993 and 1976 cm^{-1} attributed to dipole changes in the directions perpendicular and parallel to the Ga…Ga axis [31]. Thus, it is not possible to exclude the formation of H–Ga–H species by just considering the separation between these signals in our experimental data.

A close inspection of the spectra in Fig. 6 allows us to put forward that the relative percentage of each IR band at 2003 and 1980 cm^{-1} (54% and 46%, respectively) suggests the formation of terminal Ga–H bonds on coordinative unsaturated Ga surface sites (with O-vacancies) with different geometric environments. This last conclusion is further supported by an additional H_2 adsorption experiment we performed on a α-Ga_2O_3 sample, where all the Ga^{3+} ions occupy octahedral positions. For the α-Ga_2O_3, the 1980 cm^{-1} peak constituted at least 91% of the total integrated IR signal. Thus, it is possible to assign the 2003- and 1980-cm^{-1} bands to the stretching frequencies of Ga(I)–H and Ga(II)–H bonds, respectively.

The simulation of H adsorption on the β-Ga_2O_3 surface plane showed that the surface Ga–O overlap decreased while a Ga–H bond was formed either on top of a Ga(II) or Ga(I). Moreover, the Ga–H overlap was found to be 24% higher for Ga(I)–H than for Ga(II)–H, which suggest that Ga(I)–H bond is stronger than Ga(II)–H (see Table 1). This, again, is consistent with the assigned higher stretching frequency for the Ga(I)–H bond vibration.

From the computed energy vs. Ga–H distances curves and using an harmonic approximation, we have calculated the {Ga(II)–H/Ga(I)–H} frequency ratio by 1.014 ($\Delta\nu$ of 1.40%). The corresponding experimental frequency ratio is 1.012 ($\Delta\nu$ of 1.15%).

5. Conclusions

The electronic structure and bonding of hydrogen on a model for the β-Ga_2O_3(1 0 0) surface has been computed at a semiempirical level. H in not adsorbed in a clear-cut of the (1 0 0) plane, which exposes oxygens. To be active, it is necessary to introduce oxygen vacancies on the surface. After that, the exposed Ga adsorbs H being the most stable the tetra-coordinated sites. A Ga–H bond is formed at expenses of the Ga–O bond. The orbital composition of the Ga–H bond includes a Ga 4s–H 1s interaction of about 80% and Ga $4p_x$ H 1s of 20%. The DOS curves show the contribution of adsorbed H at (−17, −19) eV that is always of bonding character for both Ga(I) and Ga(II).

We have also found, that the stretching frequencies in the IR assigned to Ga(I)–H and Ga(II)–H show the same ratio than the computed force constants.

Acknowledgments

Our work was supported by UNS-Física, Fundación Antorchas and ANPCyT (PICT 12-09857 and PICT 13-07005). A. Juan, Adrian L. Bonivardi and Miguel A. Baltanás are members of

CONICET. E.A. Gonzalez, P.V. Jasen and S.E. Collins are fellows of that Institution. We thank Profs. G.J. Hutchings and D.J. Willock from Cardiff University, UK, who kindly help us with the crystal structure data.

Appendix A

The energies and optimised positions for Ga–O–H were calculated with a cluster approximation using the semiempirical molecular orbital ASED-MO method, which predicts molecular structures from atomic data (atomic wave functions and ionization potentials). This method is quite approximate, but it is used because it provides a qualitative picture of Ga–O, Ga–H and O–H interactions.

Parameters necessary for calculations are listed in Table 2. Experimental values for ionization potentials where taken from spectroscopic data [23,36].

The ASED-MO method is a modification of the Extended Hückel method that includes a repulsive term for the electrostatic interaction between nucleus [37]. The energy was computed as the difference (ΔE) between the Ga–O–H composite system when the H atom is absorbed at a specified geometry and when it is far away from the Ga–O surface. It can be expressed as Ga_2O_{3-x}

$$\Delta E_{\text{Total}} = E(\text{H–Ga}_2\text{O}_{3-x}) - E(\text{Ga}_2\text{O}_{3-x}) - E(\text{H}) + E_{\text{repulsion}}$$

where E is the electronic energy, $E_{\text{repulsion}}$ is the repulsive energy for nucleus j in the presence of a fixed atom i:

$$E_{\text{repulsion}} = \frac{1}{2}\sum_{i}\sum_{j\neq i} E_{ij}$$

Table 2
Parameters for ASED-MO calculations

Atom	Orbital	Ionization potential (eV)	Slater exponent (a.u.$^{-1}$)	Electronegativity (Pauling)
H	1s	13.60	1.000	2.1
Ga	4s	6.00	2.200	1.8
	4p	15.00	2.590	
O	2p	28.48	2.163	3.4
	2s	13.62	2.174	

(E_{ij} is a pair wise electrostatic term). The summation extends over all Ga–Ga, O–O, Ga–H and O–H pairs.

To understand the Ga–O–H interaction, we used the concept of DOS (density of states) and COOP (crystal orbital overlap population) curves implemented with the program YAeHMOP [38]. The DOS curve is a plot of the number of orbital per unit energy. The COOP curve is a plot of the overlap population weighted DOS vs. energy. The integration of the COOP curve up to the Fermi level (E_F) gives the total overlap population of the bond specified and it is a measure of the bond strength.

Due to the approximate nature of the ASED method the reported values for the energy should be interpreted in their *relative* terms.

References

[1] R. Roy, V.G. Hili, E.F. Osborn, J. Am. Chem. Soc. 74 (1952) 719.
[2] H.H. Tippins, Phys. Rev. A 316 (1965) 140.
[3] K. Bernhardt, M. Fleischer, H. Meixner, Siemens Comp. 30 (1995) 35.
[4] M.R. Lorenz, J.F. Woods, R.J. Gambino, J. Phys. Chem. Solids 28 (1967) 403.
[5] T. Harwig, G.J. Wubs, G.J. Dirksen, Solid State Commun. 18 (1976) 1223.
[6] M. Yamaga, E.G. Víllora, K. Shimamura, N. Ichinose, M. Honda, Phys. Rev. B 68 (2003) 155207.
[7] M. Fleischer, H. Meixner, Sensors Actuators B 6 (1992) 257.
[8] R. Pohle, M. Fleischer, H. Meixner, Sensors Actuators B 68 (2000) 151.
[9] T. Weh, J. Frank, M. Fleischer, H. Meixner, Sensors Actuators B 78 (2001) 202.
[10] Y. Ono, Catal. Rev. Sci. Eng. 34 (1992) 179.
[11] R. Carli, R. Le Van Mao, C. Bianchi, V. Ragaini, Catal. Lett. 21 (1993) 265.
[12] I. Takahara, M. Saito, M. Inaba, K. Murata, Catal. Lett. 96 (2004) 29.
[13] S.E. Collins, M.A. Baltanás, A.L. Bonivardi, J. Catal. 226 (2004) 410.
[14] P. Mériaudeau, C. Naccache, Appl. Catal. 73 (1991) L13.
[15] S.E. Collins, M.L. Baltanás, J.L. Garcia Fierro, A.L. Bonivardi, J. Catal. 211 (2002) 252.
[16] Ch.A. Cooper, Ch.R. Hammond, G.J. Hutchings, S.H. Taylor, D.J. Willock, K. Tabata, Catal. Today 71 (2001) 3.
[17] D. Kohl, Th. Ochs, W. Geyer, M. Fleischer, H. Meixner, Sensors Actuators B 59 (1990) 140.
[18] M. Fleischer, H. Meixner, Sensors Actuators B 6 (1992) 1728.

[19] M. Rodríguez Delgado, C. Otero Areán, Mater. Lett. 57 (2003) 2292.
[20] C. Otero Areán, A. López Bellan, M. Peñarroya Mentruit, M. Rodríguez Delgado, G. Tunes Palomino, Micropor. Mesopor. Mater. 40 (2000) 35.
[21] J.C. Lavalley, M. Daturi, V. Montouillout, G. Clet, C. Otero Areán, M. Rodríguez Delgado, A. Sahibed-dinde, Phys. Chem. 5 (2003) 1301.
[22] V.B. Kazansky, I.R. Subbotina, R.A. van Santen, E.J.M. Hensen, J. Catal. 227 (2004) 263.
[23] L. Binet, D. Gourier, C. Minot, J. Solid State Chem. 113 (1994) 420.
[24] G.C. Cabilla, A.L. Bonivardi, M.L. Baltanás, Catal. Lett. 55 (1998) 147.
[25] J.D. Ingle, S.R. Crouch, Spectrochemical Analysis, first ed., Prentice Hall, Upper Saddle River, NJ, 1988, p. 211.
[26] S. Geller, J. Chem. Phys. 33 (1960) 676.
[27] L. Pauling, The Nature of the Chemical Bond, third ed., Cornell University Press, Ithaca, New York, 1960, Chapter 13, Section 6.
[28] Z. Hajnal, J. Miró, G. Kiss, F. Réti, P. Deák, R.C. Herndon, M. Kuperberg, J. Appl. Phys. 86 (1999) 3792.
[29] H.J. Himmel, L. Manceron, A.J. Downs, P. Pullumbi, J. Am. Chem. Soc. 124 (2002) 4448.
[30] C. Liang, R.D. Davy, H.F. Schaefer III, Chem. Phys. Lett. 159 (1989) 393.
[31] C.R. Pulham, A.J. Downs, M.J. Goode, D.W.H. Rankin, H.E. Roberston, J. Am. Chem. Soc. 113 (1991) 5149.
[32] Z.L. Xiao, R.H. Hauge, J.L. Margrave, Inorg. Chem. 32 (1993) 642.
[33] A.J. Downs, M.J. Goode, C.R. Pulham, J. Am. Chem. Soc. 111 (1989) 1936.
[34] H. Qi, P.E. Gee, T. Nguyen, R.F. Hicks, Surf. Sci. 323 (1995) 6.
[35] R.H. Hauge, J.W. Kauffman, J.L. Margrave, J. Am. Chem. Soc. 102 (1980) 6005.
[36] W. Lotz, J. Opt. Soc. Am. 60 (1970) 206.
[37] A.B. Anderson, J. Chem. Phys. 62 (1975) 1187.
[38] G.A. Landrum, W.V. Glassey, Yet Another Extended Hückel Molecular Orbital Package (YAeHMOP), Cornell University, 2001, YAeHMOP extended Hückel molecular orbital package is freely available on the WWW at sourceforge.netprojects/yaehmop/.